Acta Crystallographica Section D
Biological Crystallography
ISSN 0907-4449

The role of Asp116 in the reductive cleavage of dioxygen to water in CotA laccase: assistance during the proton-transfer mechanism

Catarina S. Silva,‡ João M. Damas,‡ Zhenjia Chen, Vânia Brissos, Lígia O. Martins, Cláudio M. Soares,* Peter F. Lindley and Isabel Bento*

Instituto de Tecnologia Química e Biológica, Universidade Nova de Lisboa, Avenida da Republica, 2780-157 Oeiras, Portugal

‡ These authors contributed equally to this work.

Correspondence e-mail: claudio@itqb.unl.pt, bento@itqb.unl.pt

Received 2 November 2011
Accepted 18 December 2011

PDB References: CotA laccase, D116A mutant , 4a66; D116E mutant, 4a67; D116N mutant , 4a68.

Multi-copper oxidases constitute a family of proteins that are capable of coupling the one-electron oxidation of four substrate equivalents to the four-electron reduction of dioxygen to two molecules of water. The main catalytic stages occurring during the process have already been identified, but several questions remain, including the nature of the protonation events that take place during the reductive cleavage of dioxygen to water. The presence of a structurally conserved acidic residue (Glu498 in CotA laccase from *Bacillus subtilis*) at the dioxygen-entrance channel has been reported to play a decisive role in the protonation mechanisms, channelling protons during the reduction process and stabilizing the site as a whole. A second acidic residue that is sequentially conserved in multi-copper oxidases and sited within the exit channel (Asp116 in CotA) has also been identified as being important in the protonation process. In this study, CotA laccase has been used as a model system to assess the role of Asp116 in the reduction process of dioxygen to water. The crystal structures of three distinct mutants, D116E, D116N and D116A, produced by site-saturation mutagenesis have been determined. In addition, theoretical calculations have provided further support for a role of this residue in the protonation events.

1. Introduction

Laccases (*p*-diphenol:dioxygen oxidoreductases; EC 1.10.3.2) are the simplest members of the multi-copper oxidase (MCO) family of proteins and therefore constitute good model systems for examining structure–function relationships. Their overall three-dimensional fold comprises three cupredoxin-like domains with a type 1 (T1) copper centre located in domain 3 and a trinuclear copper centre, comprising a pair of type 3 (T3) copper ions and a type 2 (T2) copper ion, located at the interface between domains 1 and 3 (Lindley, 2001; Solomon *et al.*, 1996; Nakamura & Go, 2005; Murphy *et al.*, 1997; Fig. 1). Widely distributed in the animal, plant, fungal and bacterial kingdoms, laccases have been reported to have many different functions and to play a central role in several processes (Solomon *et al.*, 1996; Nakamura & Go, 2005; Giardina *et al.*, 2010; Mayer & Staples, 2002). Their ability to oxidize a plethora of aromatic and inorganic compounds makes them interesting and useful targets from the biotechnological processing viewpoint (Mayer & Staples, 2002; Kosman, 2010; Rodríguez Couto & Toca Herrera, 2006; Riva, 2006). The present study involves the CotA laccase from *Bacillus subtilis*, an enzyme isolated from the outer layer of the spore coat and known to be both thermostable and thermoactive (Martins *et al.*, 2002; Durão *et al.*, 2008; Enguita *et al.*, 2003).

A putative mechanism for the reduction of dioxygen to water has been proposed based on the X-ray structures of CotA laccase in different redox states (Bento *et al.*, 2005) and with adducts (Bento *et al.*, 2005; Enguita *et al.*, 2004), and by comparison of these with other reported structures of different MCOs which correspond to potential structural intermediates in the mechanism (Bento *et al.*, 2005, 2010). In addition to four electrons, the reduction process of dioxygen to water also requires four protons, which have been proposed to be facilitated by acidic residues placed within the entrance channel (Bento *et al.*, 2010; Chen *et al.*, 2010) and the exit channel (Kataoka *et al.*, 2009; Ueki *et al.*, 2006) of the enzyme (Figs. 1 and 2*a*).

The majority of MCOs have a carboxylate group from an acidic residue within the access channel to the trinuclear cluster; the exception appears to be that from *Melanocarpus albomyces*, in which the C-terminal carboxylate partially fills the channel mouth (Hakulinen *et al.*, 2002, 2008). In the CotA laccase this residue is Glu498. X-ray structure determination and biochemical data analysis of three mutants of Glu498, in which this residue is replaced by site-directed mutagenesis to an aspartate (E498D), a threonine (E498T) and a leucine (E498L), clearly indicate its proton-facilitating role; it may also exert a role in the stabilization of the reduction site as a whole (Chen *et al.*, 2010). Other studies involving site-directed mutagenesis of Glu506 in prokaryotic CueO (Kataoka *et al.*, 2009) and Glu487 in eukaryotic Fet3p (Solomon *et al.*, 2008; Augustine *et al.*, 2007) (both of which are counterparts of Glu498 in CotA laccase, but in the latter case positioned on the opposite side of the channel) strongly support the participation of a carboxylate residue as a proton donor in the dioxygen-reduction mechanism. Finally, equilibrium protonation simulations (CE/MC) of CotA laccase structures corresponding to different states of the mechanism have allowed the investigation of ionisable groups that are likely to be involved in proton-transfer mechanisms. These indicated that Glu498 is the only proton-active group in the surroundings of the trinuclear cluster in CotA (Bento *et al.*, 2010).

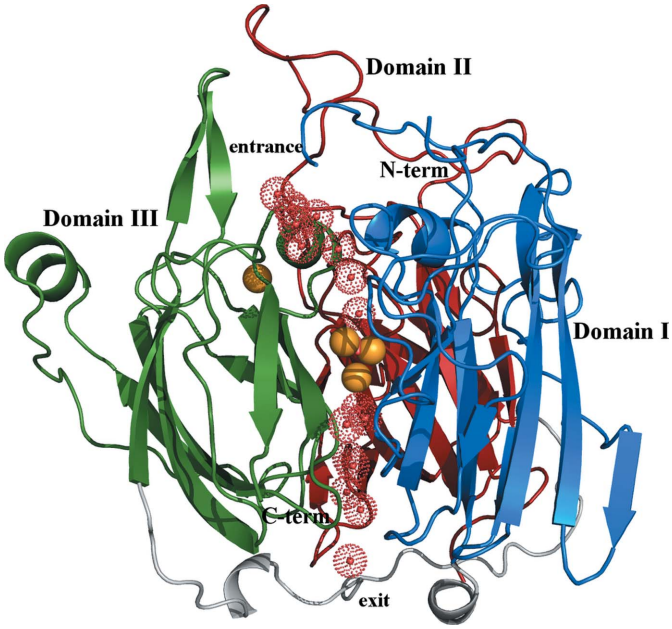

Figure 1
Three-dimensional structure of CotA laccase: overall three-dimensional fold highlighting the entrance and exit channels, above and below the trinuclear cluster, for the dioxygen and water molecules, respectively. The three cupredoxin-like domains are coloured blue (domain 1), dark red (domain 2) and green (domain 3). Cu atoms are represented as spheres coloured yellow. Substrate oxidation occurs close to the mononuclear T1 Cu centre, shuttling electrons to the trinuclear Cu centre where dioxygen reduction occurs with the concomitant release of water molecules.

In the proposed mechanism, the addition of two electrons gives rise to a peroxide moiety bound to the trinuclear cluster. The addition of two further electrons and two protons results in this dioxygen species being split into two hydroxide ions and these in turn migrate through the cluster so that they bind to the T2 copper ion but oriented into the exit channel. This migration is a key stage in the overall mechanism and is not well understood or indeed studied. It must involve a spatial displacement of the T2 copper ion, which may be consistent with it being bound by only two histidine residues and being the most labile of the copper ions. The final stages of the mechanism involve the provision of two further protons to convert the hydroxide moieties into water molecules, which can then leave the enzyme through the exit channel from the trinuclear site. Biochemical studies on mutations in other MCOs, namely Asp94 in the eukaryotic Fet3p (Solomon *et al.*, 2008; Augustine *et al.*, 2007; Quintanar *et al.*, 2005), Asp112 in the prokaryotic CueO (Kataoka *et al.*, 2009; Ueki *et al.*, 2006) and Asp105 in the fungal bilirubin oxidase (Kataoka *et al.*, 2005) from *Myrothecium verrucaria*, have already indicated the importance of an acidic residue sited within the exit channel in the mechanism. This acidic residue is not coordinated to any of the copper ions in the trinuclear centre, but the carboxylate moiety points into the channel and forms hydrogen bonds either directly or indirectly to a set of ligands belonging to or interacting with the trinuclear Cu centre.

In the present work, three distinct mutants of Asp116, the corresponding residue in CotA laccase, have been produced by site-saturation mutagenesis (Brissos *et al.*, 2012) and their crystal structures have been determined. These structures, D116E, D116N and D116A, were then used in equilibrium protonation simulations in order to further assess the role of Asp116 during the protonation process.

2. Experimental procedures

2.1. Crystallization and data collection

The CotA laccase mutants D116A, D116N and D116E were produced by site-saturation mutagenesis and batches were obtained as described elsewhere (Durão *et al.*, 2008; Brissos *et al.*, 2012). Suitable well diffracting crystals were grown for each of the CotA laccase mutants using the vapour-diffusion method at 298 K. The crystals appeared from very diverse reservoir solutions: 35% ethylene glycol (D116A), 8% PEG 6000 with 25% 2-methyl-2,4-pentanediol (MPD) in 0.1 *M* HEPES buffer pH 7.5 (D116N) and 30% dioxane in 0.1 *M*

Table 1
Data-collection statistics.

Values in parentheses are for the highest resolution shell.

	CotA mutant		
	D116A	D116N	D116E
X-ray source	In-house Bruker AXS MICROSTAR	In-house Bruker AXS MICROSTAR	ESRF ID23-EH1
Wavelength (Å)	1.544	1.544	0.975
Detector	PLATINUM 135 CCD	PLATINUM 135 CCD	ADSC Quantum Q315r
Crystal-to-detector distance (mm)	85.0	85.0	305.4
Resolution (Å)	1.95 (2.0–1.95)	2.0 (2.05–2.00)	2.1 (2.21–2.10)
Space group	$P3_121$	$P3_121$	$P3_121$
Unit-cell parameters (Å)	a = 101.7, c = 136.6	a = 101.6, c = 136.7	a = 101.7, c = 136.8
No. of unique hkl	60037 (8283)	55571 (7488)	46481 (15233)
Completeness (%)	100.0 (99.9)	99.8 (100.0)	96.3 (90.0)
Mean $I/\sigma(I)$	17.5 (3.4)	12.4 (2.7)	12.6 (2.9)
$R_{\rm merge}$	0.047 (0.290)	0.059 (0.358)	0.049 (0.254)
Multiplicity	5.3 (4.0)	4.5 (3.3)	3.0 (2.4)

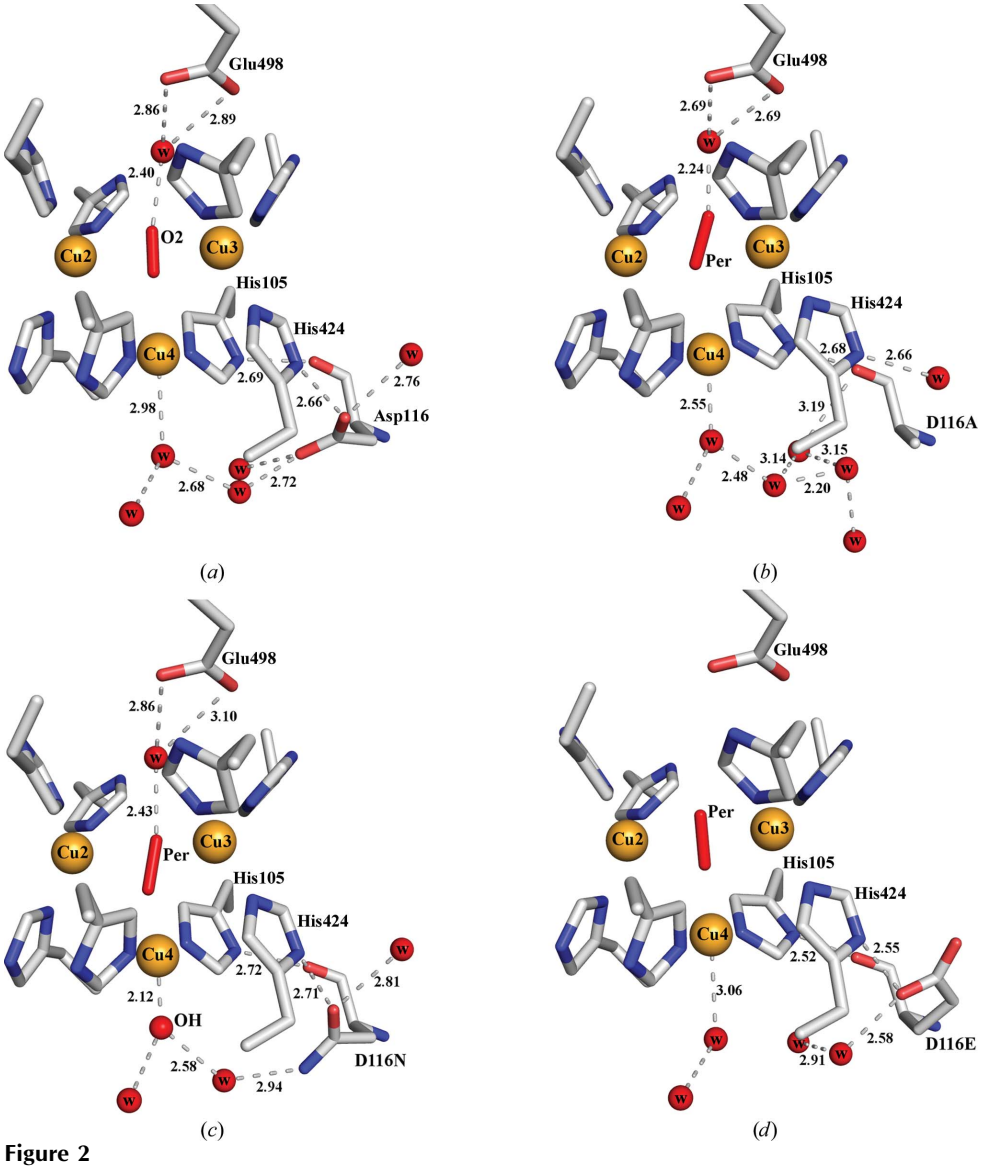

Figure 2
Structural detail of the CotA trinuclear centre and its neighbourhood. The acidic residues Glu498 and Asp116 are highlighted. (*a*) Native CotA, (*b*) D116A, (*c*) D116N and (*d*) D116E. Cu ions are represented as yellow spheres.

HEPES buffer pH 7.5 (D116E). Drops were set up by the combination of 1.5 µl protein sample (at concentrations of 25 mg ml^{-1} for both D116A and D116N, and 50 mg ml^{-1} for D116E in 20 m*M* Tris–HCl pH 7.6) with the reservoir solution in a 1:1 ratio. Crystals were directly flash-cooled in liquid nitrogen prior to data collection, with no additional cryogenic agent added to the aforementioned crystallization solutions as they themselves constitute cryogenic conditions.

Diffraction data were collected under a cold nitrogen stream at 100 K on the ID23-EH1 beamline, ESRF, Grenoble for the D116E mutant and using an in-house Bruker AXS MICROSTAR imaging-plate detector (X8 PROTEUM diffractometer) for the D116A and D116N mutants. The crystals of the D116A, D116N and D116E mutants diffracted to 1.95, 2.0 and 2.1 Å resolution, respectively, and belonged to the trigonal space group $P3_121$ with one single molecule per asymmetric unit.

Data sets were processed and the intensities were scaled using *MOSFLM* (Leslie, 2006) and *SCALA* from the *CCP*4 suite (Winn *et al.*, 2011) for the D116E mutant or using the programs *SAINT* and *SADABS*, respectively, as part of the Bruker AXS *PROTEUM* software suite with data statistics obtained using *XPREP* (Bruker AXS) for the D116A and D116N mutants. Data-collection details and processing statistics are presented in Table 1.

2.2. Structure determination and refinement

For all three CotA laccase mutants, the structure was solved by the molecular-replacement method using the coordinates of the native CotA laccase (PDB entry 1w6l; Bento *et al.*, 2005) as the initial search model, from

which all solvent atoms and heteroatoms had previously been removed. Molecular replacement was carried out using *MOLREP* (Vagin & Teplyakov, 2010) from the *CCP*4 program suite (Winn *et al.*, 2011), yielding single solutions with typical correlation coefficients and *R* factors of approximately 71% and 42%, respectively, for all three mutants. The positions of all four Cu atoms became evident in the electron-density synthesis maps after a few refinement cycles. Refinement was then pursued using the maximum-likelihood functions in *REFMAC* (Murshudov *et al.*, 2011) from the *CCP*4 program suite (Winn *et al.*, 2011). Careful observation of the σ_A-weighted $2|F_o| - |F_c|$ and $|F_o| - |F_c|$ maps throughout cycles of model building and manual fitting in *Coot* (Emsley & Cowtan, 2004) allowed improvement of the models. After a few rounds of refinement, solvent molecules were placed in the model obeying geometrical and stereochemical restraints. Molecules of ethylene glycol were also located in the D116A mutant, and molecules of HEPES buffer and MPD were modelled for the D116N mutant. Isotropic refinement of the atomic displacement parameters was also performed for all of the atoms present in the model. Full occupancy was assigned to all four copper ions on the basis that their isotropic thermal vibration parameters refined approximately to those of the ligand atoms to which they were bound. Determination of the species located between the two T3 Cu atoms was achieved by a combination of cautious use of OMIT and standard difference Fourier synthesis and inspection of thermal vibration coefficients throughout refinement, as described previously (Bento *et al.*, 2010). Modelling of monoatomic (chlorine ion and monoatomic oxygen species such as hydroxide) and diatomic (peroxide and a dioxygen molecule) species into the positive ovoid-like electron-density peak indicated that a peroxide moiety is the entity that best refines for all three mutants (Supplementary Fig. S1[1]). This species constitutes the peroxide intermediate, which is considered to be an O_2^{2-} moiety throughout the paper, in accordance with the proposed mechanism (Bento *et al.*, 2005, 2010; see §4). The separation distance between Cu2 and Cu3 is 4.58, 4.63 and 4.74 Å in the D116A, D116N and D116E mutants, respectively, resembling that in the peroxide-soaked structure of CotA laccase (Bento *et al.*, 2005).

Table 2
Refinement statistics and quality of the refined models.

	CotA mutant		
	D116A	D116N	D116E
No. of protein atoms	4098	4058	4084
No. of solvent atoms	494 (11 EDO)	478 (1 HEPES + 2 MPD)	435
No. of heteroatoms	4 Cu + 2 O	4 Cu + 3 O	4 Cu + 2 O
Final *R* factor	0.174	0.169	0.183
Final free *R* factor (reflections used)	0.203 (5.0%)	0.200 (5.1%)	0.220 (5.1%)
Mean *B* values (Å^2)			
Protein	19.86	18.99	31.34
Solvent	28.77	28.29	38.60
Overall	20.82	19.96	32.03
Estimated overall coordinate uncertainty† (Å)	0.086	0.087	0.124
Distance deviations‡			
Bond distances (Å)	0.017	0.015	0.021
Bond angles (Å)	1.428	1.453	1.501
Planar groups (Å)	0.008	0.008	0.008
Chiral volume deviation (Å^3)	0.107	0.105	0.109
Model quality			
Ramachandran analysis§ (%)			
Favourable	96.6 (478)	97.2 (484)	97.20 (484)
Generous	3.0 (15)	2.8 (14)	2.8 (14)
Disallowed	0.4 (2)	0.0 (0)	0.0 (0)

† Based on maximum likelihood. ‡ R.m.s. deviations from standard values. § Determined using *RAMPAGE* (Winn *et al.*, 2011). Values in parentheses are the numbers of residues.

Similarly to other reported structures of CotA, the loop region comprising residues 89–97 is very poorly defined and therefore not entirely modelled in the three mutants. Likewise, additional electron density was observed in the area surrounding Cys35 (Chen *et al.*, 2010); this was modelled as an oxidized cysteine residue for the D116E mutant, while for the remaining mutants, D116N and D116A, the cysteine side chain was modelled, with two alternate conformations in the latter case. Model validation was monitored using *RAMPAGE* from the *CCP*4 suite (Winn *et al.*, 2011). The coordinates and structure factors have been deposited in the PDB as entries 4a66, 4a67 and 4a68 for the D116A, D116E and D116N mutants, respectively.

Refinement statistics and details of the final quality of the models are listed in Table 2. Figs. 1 and 2 and Supplementary Fig. S1 were drawn with *PyMOL* (DeLano, 2002).

2.3. Theoretical calculations

Using the X-ray structures of the Asp116 mutants, simulated pH titrations have been made using continuum electrostatic/Monte Carlo (CE/MC) methods. These calculations use semi-rigid structures owing to the employment of tautomers (see below); consequently, poorly defined regions of the structure were treated in an identical manner for all three mutants. This procedure is carefully explained in Bento *et al.* (2010). Additionally, and since the bound peroxides occupy slightly different positions (although contained within the estimated error of the coordinates), which can generate substantial electrostatic differences owing to the point-charge nature of the parameterization, it was decided to use the peroxide species of the CotA–H_2O_2 structure (Bento *et al.*, 2005). These choices for the mutant models help to minimize

[1] Supplementary material has been deposited in the IUCr electronic archive (Reference: DZ5245). Services for accessing this material are described at the back of the journal.

the bias that different positions of the ligand may have on the comparisons between the titration curves calculated for the mutants and for the native enzyme. Additionally, the trinuclear centre was considered to be in the same state, which means that the hydroxyl bound to the T2 copper centre in the D116N mutant was considered to be a water molecule in the calculations. This decision was also aimed at reducing the bias by maintaining the consistency of the trinuclear centre.

The CE/MC methodology which we have developed considers different tautomeric positions for the ionisable groups and also alternative positions for the protons of the OH moieties of Ser and Thr residues. This is a necessity in order to improve the rigid nature of CE calculations. In CE methods the protein can be treated as a low-dielectric model immersed in a high dielectric corresponding to the solvent, with charges placed at atomic positions with a given atomic radii. The dielectric constants used were 80 for the solvent and 10 for the protein, which are values that reproduce experimental data well within the realm of the parameterization used (Teixeira *et al.*, 2005). Sets of partial charges and atomic radii were taken from the 43A1 GROMOS96 force field (van Gunsteren *et al.*, 1996; Scott *et al.*, 1999), except for the T1 copper and the trinuclear metal centres, for which partial charges were derived using quantum-chemical calculations as described previously (Bento *et al.*, 2010). The package *MEAD* v.2.2.0 (Bashford & Gerwert, 1992) was used for the CE calculations, with a solvent-probe radius of 1.4 Å, an ion-exclusion layer of 2.0 Å, an ionic strength of 0.1 *M* and a temperature of 300 K. The obtained individual and interaction terms of the binding free energy of the protons were then used in sampling of the binding states of the protons. The program *PETIT* v.1.3 (Baptista & Soares, 2001; Teixeira *et al.*, 2002) was used for the MC sampling of the protonation states, with averages computed using 10^5 MC steps. Site pairs were selected for double moves when at least one pairwise term was greater than 2 pK units.

3. Results

3.1. Structural characterization of the mutants

Crystal structure comparison of the three Asp116 mutant enzymes with the native CotA laccase structure shows no significant differences in terms of the overall three-dimensional fold. Superposition of the Cα traces of each mutant onto the fully loaded native CotA structure (PDB entry 1w6l; Bento *et al.*, 2005) yielded r.m.s. deviation values of 0.24, 0.17 and 0.16 Å for the D116A, D116N and D116E mutants, respectively. A few minor changes were observed in some of the external loop regions such as that composed of residues 212–219, for which the D116A mutant showed the most pronounced shift relative to the backbone chain. Additionally, the loop comprising residues 357–364 was found to have very poorly defined electron density in this mutant, which did not allow complete modelling. Within this loop is Tyr358, which was found to have a modification at position CD2 that was not modelled in this structure as no satisfactory fit to the electron density was achieved.

With respect to the copper centres, no significant changes were observed at the T1 copper centre, which shows full occupancy in all three mutants. At the trinuclear centre, full occupancy was observed for the copper ions and for the diatomic species in between the T3 copper ions. This moiety was modelled as a peroxide species in all of the mutants. In a similar manner to the native enzyme, this species interacts with a solvent molecule, which in turn hydrogen bonds to the side chain of Glu498, although this water is only weakly defined in the D116E mutant (and hence was not modelled). The reasons for the absence of such a solvent molecule in the latter mutant are not clear, with such an absence only being reported for the reduced state of native CotA (Bento *et al.*, 2005).

In the native enzyme, Asp116 is sited within the exit channel in close proximity to the T2 Cu ion in the trinuclear centre (Fig. 2*a*). Its backbone carbonyl O atom forms a hydrogen bond to the ND1 atom of His105 (2.69 Å), a ligand bound to the T2 site. On the other hand, its carboxylate side chain forms hydrogen bonds to both the ND1 atom of His424 (2.66 Å), a ligand bound to one of the T3 Cu ions, and a solvent molecule (2.72 Å) which is part of a chain of waters oriented between the T2 Cu and the surface of the CotA molecule. In the case of the D116A (Fig. 2*b*) and D116N (Fig. 2*c*) mutants, in which the negatively charged aspartate has been mutated to an apolar alanine and a polar uncharged asparagine, respectively, the residue side chains remain oriented into the exit channel and the water network that interacts with the T2 Cu is maintained. In the D116A mutant two water molecules occupy the vacant side-chain site, essentially mimicking the carboxylate O atoms with respect to hydrogen bonding and extending the water network. The mutated alanine is no longer able to establish hydrogen bonds through its side chain and hence does not interact with His424. In fact, a water molecule placed near the His424 ring in the native structure has adjusted its position in the D116A mutant, directly interacting with the ring. In the D116N mutant the side chain of the asparagine residue is slightly shifted with respect to the aspartate of the native protein, but still maintains hydrogen bonds to the histidines binding to the T3 and T2 Cu ions. It also interacts with Thr111, which has its side chain oriented towards the exit channel (ND2–OG1, 3.07 Å). Moreover, in this mutant the T2 Cu is directly bound to a hydroxyl species with a Cu4–OH distance of 2.12 Å.

On the other hand, in the D116E mutant (Fig. 2*d*), in which a negatively charged residue has been maintained at the aspartate position, the longer length of the side chain causes it to rotate towards the interior of the protein, with a concomitant change in the water network that interacts with the T2 Cu ion. The glutamate side chain still hydrogen bonds to water molecules, but these are some 4 Å away from the water molecule hydrogen-bonded to the T2 copper ion. This conformational movement of the side chain increases the distance of the carboxylate moiety from the T2 copper and it is therefore expected that its efficiency in mediating or assisting

protonation of hydroxyl groups bound to the T2 copper ion is decreased. As in D116N, this mutant remains hydrogen-bonded to both His424 and His105, the former through the OE2 atom and the latter through the main-chain carbonyl moiety.

In all three mutants, the presence of a peroxide species between the T3 Cu ions indicates that a cycle of the reaction has been initiated.

3.2. Titration profiles of Glu498 in the Asp116 mutants

Previously reported protonation equilibrium simulations using CE/MC methods showed that Glu498 is the only proton-active residue (*i.e.* that actively titrates in the physiological pH range; protonation between 0.05 and 0.95) in the surroundings of the trinuclear centre (Bento *et al.*, 2010). Furthermore, these simulations showed that Glu498 was deprotonated in native oxidized holo-CotA around pH 7, increasing its protonation in the peroxide intermediate and reduced state. In contrast, Asp116 was found to be essentially deprotonated in the active pH range of the enzyme in all of the states analysed (Bento *et al.*, 2010).

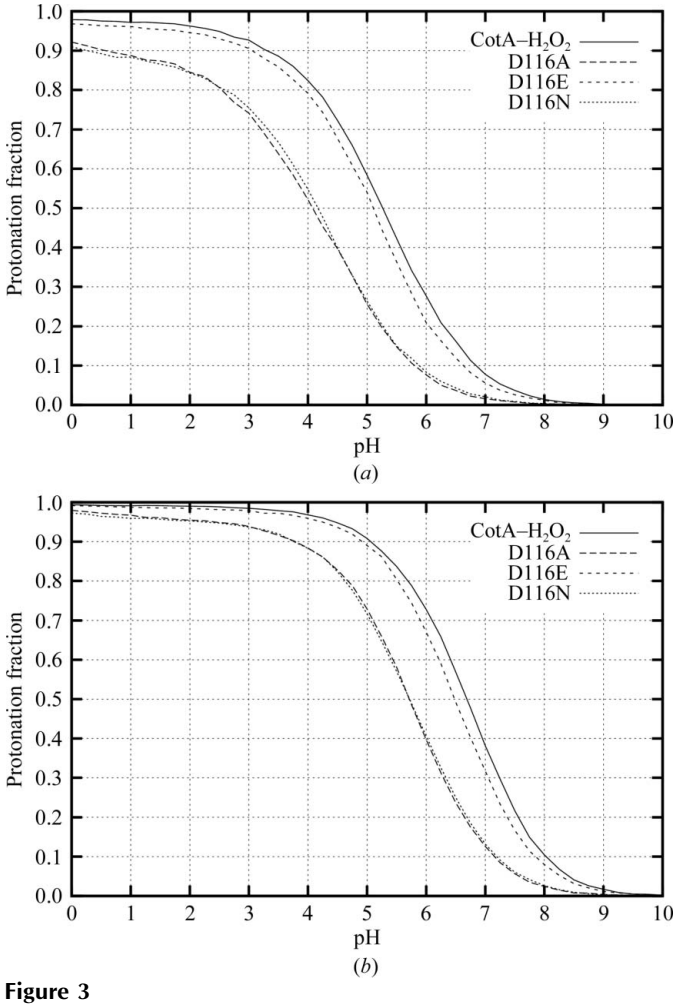

Figure 3
Simulated pH titrations of Glu498 for the CotA–H_2O_2 state (Bento *et al.*, 2005) and the three D116 mutants (*a*) with T1 copper centre oxidized and (*b*) with T1 copper centre reduced.

In the present study, with the aim of evaluating the role of Asp116 in the CotA laccase protonation process, the pH titration has again been simulated for all titratable groups using the determined structures of the D116A, D116E and D116N mutants. The previous conclusions remain valid (Bento *et al.*, 2010) and in all cases Glu498 remains the only proton-active residue in the surroundings of the trinuclear centre. However, changes in its protonation are observed, with a pK_a shift of ∼1 unit in the titration profile of Glu498 when comparing the D116A and D116N mutants with the native enzyme (Fig. 3). In contrast, the titration profile of Glu498 in the D116E mutant shifted only very slightly, suggesting that Glu498 retains its protonating capabilities in this mutant. Note that the titration properties of the glutamate residue in the D116E mutant are very similar to those of the aspartate in the native CotA (Bento *et al.*, 2010), indicating that the titration profile of this glutamate changes only very slightly and that the residue remains completely deprotonated at pH ranges around pH 7 (results not shown). These results are quite surprising and indicate that the presence of a negative charge in position 116 is a strong controlling factor in the protonation of Glu498; the physical basis relies on a long-range electrostatic effect between this negative charge and the protonation of Glu498, which is effectively stabilized and maintained ready for protonation of the initial dioxygen species. This electrostatic effect is stronger because it occurs in the protein interior. The elimination of this negative charge by mutation to Ala or to Asn has a substantial effect on the titration profile of Glu498 by lowering its protonation probability. Finally, these relative shifts in the titration profiles are independent of the T1 copper centre redox state (compare Figs. 3*a* and 3*b*), which also has an effect on the titration of Glu498 but does not change the relative effect of the mutations.

4. Discussion

Previous studies on CotA (Bento *et al.*, 2010) indicated that Glu498 in the entrance channel is the only proton-active group in the neighbourhood of the trinuclear centre; indeed, mutations of this residue (Chen *et al.*, 2010) resulted in a catalytically compromised (E498D) or dead enzyme (E498T and E498L). In contrast, Asp116 in the exit channel has been suggested by these studies to be fully ionized in all physiological situations (Bento *et al.*, 2010). Recent kinetic studies by Brissos *et al.* (2012) on mutants of Asp116 (D116A, D116N and D116E) showed that their catalytic properties have been severely compromised, with the decrease in activity being mainly associated with the turnover of the enzymes. In enzymatic assays performed with 2,6-DMP (2,6-dimethoxyphenol) in the pH range 7–8 (Brissos *et al.*, 2012), a pH similar to our crystallization conditions (pH 7.5), the Asp116 mutants showed turnover-number differences of 10^3 and 10^4 for D116A and D116N, respectively, and around 70-fold for D116E when compared with native CotA. Similar assays performed in the pH range 3–4 with ABTS showed a decrease of only around one order of magnitude for all mutants.

Clearly, the presence of an aspartate at position 116 is important for catalysis and the present results suggest that a negative charge at this position may be critical for the protonation mechanisms of the dioxygen-reduction process. The absence of this negative charge in the D116A and D116N mutants causes no significant structural changes at the trinuclear site, with the water network that interacts with the T2 Cu being maintained (Figs. 2*b* and 2*c*); however, it causes a pK_a downshift in the Glu498 simulated protonation profile (Fig. 3*a*) and a peroxide intermediate is observed in the crystal structures of both mutants (Figs. 2*b* and 2*c*). On the other hand, in the D116E mutant, in which the negative charge is maintained, the water-network connectivity near the T2 site is perturbed (Fig. 2*d*) and a peroxide intermediate is still observed in its crystal structure. However, in this case the protonation profiles for both Glu116 and Glu498 did not change, remaining similar to those observed for the native enzyme. As Glu498 is under comparable electrostatic influences in the D116E mutant and in the native enzyme, one could expect similar proton provision to the catalytic cycle in both situations. Yet, the D116E mutant is only capable of retaining residual activity. Together, these results seem to indicate that Asp116 not only has a role as a negative charge, controlling the protonation characteristics of Glu498, but may also be fundamental to maintain the connectivity of the water network in the vicinity of the T2 Cu (compare Figs. 2*a* and 2*d*). Another important role may involve proton-transfer kinetics, which cannot be addressed using the current methodology.

Furthermore, in the light of the proposed mechanism (Bento *et al.*, 2005, 2010), if the protonation of the dioxygen species bound between the T3 Cu ions is incomplete it will affect the formation of hydroxide ions and consequently the rest of the catalytic mechanism. The resolved structures show that the Asp116 mutants are in a peroxide intermediate state, with the experimental starting point of the enzyme corresponding to the reduced state (owing to microaerophilic cell-growth conditions; Durão *et al.*, 2008; Brissos *et al.*, 2012), binding dioxygen as soon as it becomes available. This means that catalysis has been prevented from proceeding further, with the D116A and D116N mutants arrested in the peroxide intermediate state (Figs. 2*b* and 2*c*), in agreement with the fact that these mutants are catalytically dead (Brissos *et al.*, 2012). In the structure of the D116E mutant the peroxide intermediate state was also captured (Fig. 2*d*), which is natural given that the activity of this mutant is almost nonexistent (Brissos *et al.*, 2012), increasing the probability of this state being found. This peroxide intermediate state has only been reported in T1-depleted or inactive enzymes (Kataoka *et al.*, 2005, 2009; Augustine *et al.*, 2007; Palmer *et al.*, 2001), in peroxide-soaked structures (Bento *et al.*, 2005; Messerschmidt *et al.*, 1993), in the M502F mutant of CotA (Durão *et al.*, 2006) and in the blue laccase from *Lentinus tigrinus* (Ferraroni *et al.*, 2007), but in this latter case the crystals had been exposed to high X-ray radiation doses under aerobic conditions and high pH.

Similar studies on Asp116-counterpart mutants have been reported in other laccases. The mutations reported by Kataoka *et al.* (2005) of Asp105 of the fungal bilirubin oxidase (BO) from *M. verrucaria* showed comparable results at high pH values (pH 8.4), with a decreased catalytic activity for the D105E variant and a practically nonexistent or null activity for the D105A and D105N mutants, respectively. Furthermore, a structural role was also suggested for the aspartate residue, as the removal of the negatively charged moiety in D105A and D105N resulted in some copper depletion and an inability to reincorporate it under anaerobic conditions (Kataoka *et al.*, 2005). Such a structural role in the integrity of the trinuclear cluster is not evident in the case of CotA laccase. Mutation of the equivalent Asp (Asp94) residue in yeast Fet3p (Quintanar *et al.*, 2005) to Ala (D94A) or Asn (D94N) resulted in significant electronic changes at the trinuclear site, and the enzyme became unreactive towards dioxygen. On the other hand, mutation to Glu (D94E) produced only minor electronic changes at the trinuclear site, rendering an enzyme that was still active (although with a slower decay of the peroxide intermediate). For the bacterial laccase CueO, mutations of the equivalent Asp112 residue yielded a significant catalytic impairment at pH 5.5 for all three variants D112E, D112A and D112N, although much more severe for the latter two, as reported by Ueki *et al.* (2006).

Altogether, it is evident that an aspartate at position 116 in CotA is important for catalysis, either by modulating the protonation events or by maintaining the local geometry and water connectivity at the trinuclear copper site. In fact, it appears that these sites are fine-tuned for proper catalysis (Yoon *et al.*, 2009), which further supports the concept that even subtle perturbations in its surroundings, such as that observed in the D116E mutant, may compromise the entire catalytic process. Finally, we propose that, unlike the effect of mutations of Glu498, which catalytically kill the enzyme activity (Chen *et al.*, 2010), the effect of mutating Asp116 tunes the catalytic properties of the enzyme, since at low pH values Glu498 may be in a protonation state of interest to the catalysis and the enzyme is still able to catalyse dioxygen reduction to some extent; hence, the differences between the catalysis with 2,6-DMP (at pH 7–8) and ABTS (at pH 3–4). This research has therefore clarified the respective roles of Asp116 and Glu498 in the mechanism of dioxygen reduction by CotA, but one outstanding question remains to be addressed. This concerns the mechanism by which the hydroxyl species or water molecules produced during the catalytic process pass through the T2 Cu into the exit channel and clearly requires further study.

Maria Arménia Carrondo is gratefully acknowledged for support. The European Synchrotron Radiation Facility, Grenoble, France and the Macromolecular Crystallography staff are sincerely acknowledged for provision of synchrotron-radiation facilities and support. This work was supported by a project grant from the European Union (BIORENEW, FP6-2004-NMP-NI-4/026456) and by Fundação para a Ciência e Tecnologia through grant PEst-OE/EQB/LA0004/2011. CSS and JMD hold PhD fellowships (SFRH/BD/40586/2007 and

SFRH/BD/41316/2007, respectively) and ZC and VB hold postdoctoral fellowships (SFRH/BPD/27104/2006 and SFRH/BPD/46808/2008, respectively) from Fundação para a Ciência e Tecnologia, Portugal.

References

Augustine, A. J., Quintanar, L., Stoj, C. S., Kosman, D. J. & Solomon, E. I. (2007). *J. Am. Chem. Soc.* **129**, 13118–13126.

Baptista, A. M. & Soares, C. M. (2001). *J. Phys. Chem. B*, **105**, 293–309.

Bashford, D. & Gerwert, K. (1992). *J. Mol. Biol.* **224**, 473–486.

Bento, I., Martins, L. O., Lopes, G. G., Carrondo, M. A. & Lindley, P. F. (2005). *Dalton Trans.*, pp. 3507–3513.

Bento, I., Silva, C. S., Chen, Z., Martins, L. O., Lindley, P. F. & Soares, C. M. (2010). *BMC Struct. Biol.* **10**, 28.

Brissos, V., Chen, Z. & Martins, L. O. (2012). Submitted.

Chen, Z., Durão, P., Silva, C. S., Pereira, M. M., Todorovic, S., Hildebrandt, P., Bento, I., Lindley, P. F. & Martins, L. O. (2010). *Dalton Trans.* **39**, 2875–2882.

DeLano, W. L. (2002). *PyMOL*. http://www.pymol.org.

Durão, P., Bento, I., Fernandes, A. T., Melo, E. P., Lindley, P. F. & Martins, L. O. (2006). *J. Biol. Inorg. Chem.* **11**, 514–526.

Durão, P., Chen, Z., Fernandes, A. T., Hildebrandt, P., Murgida, D. H., Todorovic, S., Pereira, M. M., Melo, E. P. & Martins, L. O. (2008). *J. Biol. Inorg. Chem.* **13**, 183–193.

Emsley, P. & Cowtan, K. (2004). *Acta Cryst.* D**60**, 2126–2132.

Enguita, F. J., Marçal, D., Martins, L. O., Grenha, R., Henriques, A. O., Lindley, P. F. & Carrondo, M. A. (2004). *J. Biol. Chem.* **279**, 23472–23476.

Enguita, F. J., Martins, L. O., Henriques, A. O. & Carrondo, M. A. (2003). *J. Biol. Chem.* **278**, 19416–19425.

Ferraroni, M., Myasoedova, N. M., Schmatchenko, V., Leontievsky, A. A., Golovleva, L. A., Scozzafava, A. & Briganti, F. (2007). *BMC Struct. Biol.* **7**, 60.

Giardina, P., Faraco, V., Pezzella, C., Piscitelli, A., Vanhulle, S. & Sannia, G. (2010). *Cell. Mol. Life Sci.* **67**, 369–385.

Gunsteren, W. F. van, Billeter, S. R., Eising, A. A., Hunenberger, P. H., Kruger, P., Mark, A. E., Scott, W. R. P. & Tironi, I. G. (1996). *Biomolecular Simulation: The GROMOS96 Manual and User Guide.* Zurich: Verlag der Fachvereine Hochschulverlag AG an der ETH Zurich.

Hakulinen, N., Andberg, M., Kallio, J., Koivula, A., Kruus, K. & Rouvinen, J. (2008). *J. Struct. Biol.* **162**, 29–39.

Hakulinen, N., Kiiskinen, L. L., Kruus, K., Saloheimo, M., Paananen, A., Koivula, A. & Rouvinen, J. (2002). *Nature Struct. Biol.* **9**, 601–605.

Kataoka, K., Kitagawa, R., Inoue, M., Naruse, D., Sakurai, T. & Huang, H. (2005). *Biochemistry*, **44**, 7004–7012.

Kataoka, K., Sugiyama, R., Hirota, S., Inoue, M., Urata, K., Minagawa, Y., Seo, D. & Sakurai, T. (2009). *J. Biol. Chem.* **284**, 14405–14413.

Kosman, D. J. (2010). *J. Biol. Inorg. Chem.* **15**, 15–28.

Leslie, A. G. W. (2006). *Acta Cryst.* D**62**, 48–57.

Lindley, P. F. (2001). *Multi-Copper Oxidases.* Basel, New York: Marcel Dekker, Inc.

Martins, L. O., Soares, C. M., Pereira, M. M., Teixeira, M., Costa, T., Jones, G. H. & Henriques, A. O. (2002). *J. Biol. Chem.* **277**, 18849–18859.

Mayer, A. M. & Staples, R. C. (2002). *Phytochemistry*, **60**, 551–565.

Messerschmidt, A., Luecke, H. & Huber, R. (1993). *J. Mol. Biol.* **230**, 997–1014.

Murphy, M. E., Lindley, P. F. & Adman, E. T. (1997). *Protein Sci.* **6**, 761–770.

Murshudov, G. N., Skubák, P., Lebedev, A. A., Pannu, N. S., Steiner, R. A., Nicholls, R. A., Winn, M. D., Long, F. & Vagin, A. A. (2011). *Acta Cryst.* D**67**, 355–367.

Nakamura, K. & Go, N. (2005). *Cell. Mol. Life Sci.* **62**, 2050–2066.

Palmer, A. E., Lee, S. K. & Solomon, E. I. (2001). *J. Am. Chem. Soc.* **123**, 6591–6599.

Quintanar, L., Stoj, C., Wang, T.-P., Kosman, D. J. & Solomon, E. I. (2005). *Biochemistry*, **44**, 6081–6091.

Riva, S. (2006). *Trends Biotechnol.* **24**, 219–226.

Rodríguez Couto, S. & Toca Herrera, J. L. (2006). *Biotechnol. Adv.* **24**, 500–513.

Scott, W. R. P., Hünenberger, P. H., Tironi, I. G., Mark, A. E., Billeter, S. R., Fennen, J., Torda, A. E., Huber, T., Krüger, P. & van Gunsteren, W. F. (1999). *J. Phys. Chem.* **103**, 3596–3607.

Solomon, E. I., Augustine, A. J. & Yoon, J. (2008). *Dalton Trans.*, pp. 3921–3932.

Solomon, E. I., Sundaram, U. M. & Machonkin, T. E. (1996). *Chem. Rev.* **96**, 2563–2606.

Teixeira, V. H., Cunha, C. A., Machuqueiro, M., Oliveira, A. S., Victor, B. L., Soares, C. M. & Baptista, A. M. (2005). *J. Phys. Chem. B*, **109**, 14691–14706.

Teixeira, V. H., Soares, C. M. & Baptista, A. M. (2002). *J. Biol. Inorg. Chem.* **7**, 200–216.

Ueki, Y., Inoue, M., Kurose, S., Kataoka, K. & Sakurai, T. (2006). *FEBS Lett.* **580**, 4069–4072.

Vagin, A. & Teplyakov, A. (2010). *Acta Cryst.* D**66**, 22–25.

Winn, M. D. (2011). *Acta Cryst.* D**67**, 235–242.

Yoon, J., Fujii, S. & Solomon, E. I. (2009). *Proc. Natl Acad. Sci. USA*, **106**, 6585–6590.